

Altered expression of nuclear and cytoplasmic histone H1 in pulmonary artery and pulmonary artery smooth muscle cells in patients with IPAH

Megha Talati¹, Erin Seeley², Kaori Ihida-Stansbury³, Horace Delisser³, Hayes McDonald², Fei Ye⁴, Xueqiong Zhang⁴, Yu Shyr⁴, Richard Caprioli², and Barbara Meyrick⁵

¹Departments of Medicine and ²Chemistry, Vanderbilt University Medical Center, Nashville, Tennessee, USA, ³Department of Medicine and Pathology and Laboratory Medicine, University of Pennsylvania, Philadelphia, Pennsylvania, USA, ⁴Departments of Biostatistics and Pathology, ⁵Microbiology and Immunology, Vanderbilt University Medical Center, Nashville, Tennessee, USA
Drs. Talati and Seeley contributed equally for this manuscript

ABSTRACT

The pathogenesis of idiopathic pulmonary hypertension is poorly understood. This paper utilized histology-based Matrix-Assisted Laser Desorption Ionization Mass Spectrometry (MALDI MS) to identify as-yet unknown proteins that may be associated with the structural changes in the pulmonary arterial walls of patients with IPAH. The technology identified significant increases in two fragments of histone H1 in the IPAH cases compared to controls. This finding was further examined using immunofluorescence techniques applied to sections from IPAH and control pulmonary arteries. In addition, cultured pulmonary artery smooth muscle cells (PASCs) were utilized for Western analysis of histone H1 and importin β and importin 7, immunoprecipitation and assessment of nucleosomal repeat length (NRL). Immunofluorescence techniques revealed that nuclear expression of histone H1 was decreased and the chromatin was less compact in the IPAH cases than in the controls; furthermore, some cases showed a marked increase in cytoplasmic histone H1 expression. Using nuclear and cytoplasmic fractions of cultured PASCs, we confirmed the reduction in histone H1 in the nucleus and an increase in the cytoplasm in IPAH cells compared to controls. Immunoprecipitation demonstrated a decreased association of histone H1 with importin β while importin 7 was unchanged in the IPAH cells compared to controls. The assessment of NRL revealed that the distance between nucleosomes was increased by ~20 bp in IPAH compared to controls. We conclude that at least two factors contribute to the reduction in nuclear histone H1—fragmentation of the protein and decreased import of histone H1 into the nucleus by importins. We further suggest that the decreased nuclear H1 contributes the less compact nucleosomal pattern in IPAH and this, in turn, contributes to the increase in NRL.

Key Words: idiopathic pulmonary arterial hypertension, importins, linker histones, matrix-assisted laser desorption ionization mass spectrometry, nucleosomal repeat length

Idiopathic pulmonary arterial hypertension (IPAH) is a rare but devastating disease that mainly affects young female adults, and when left untreated leads to death within three to four years of diagnosis. Histological examination of the lungs of these patients reveals a number of characteristic changes in, or remodeling of, the pulmonary arterial bed. For example, in the small intraacinar arteries, changes include appearance of muscle in smaller and more peripheral arteries as compared to normal, concentric, and eccentric intimal thickening, and obliteration of the lumen, all changes that

doubtlessly contribute to the increase in pulmonary arterial pressure.^[1,2]

To date, the expression of a number of proteins has been linked with the development and maintenance of PAH. For example, using immunohistochemical and in situ hybridization techniques, endothelial cells in plexiform lesions have been shown to express VEGF mRNA and

Address correspondence to:

Dr. Barbara Meyrick

Department of Pathology, Microbiology and Immunology
Vanderbilt University Medical Center
Nashville, TN 37232-2650, USA
Email: barbara.meyrick@vanderbilt.edu

Access this article online

Quick Response Code:



Website: www.pulmonarycirculation.org

DOI: 10.4103/2045-8932.101645

How to cite this article: Talati M, Seeley E, Ihida-Stansbury K, Delisser H, McDonald H, Ye F, et al. Altered expression of nuclear and cytoplasmic histone H1 in pulmonary artery and pulmonary artery smooth muscle cells in patients with IPAH. *Pulm Circ* 2012;2:340-51.

protein and the mRNA and protein of VEGFR-2.^[3] Medium- and small-size pulmonary arteries from patients with IPAH show increased expression of FLAP (5-LO activating protein) when compared to normal individuals.^[4] Increased expression of the extracellular matrix protein tenascin-C has been demonstrated in the adventitia and subendothelial region of arteries with hypertrophic walls and in obstructed arteries.^[5,6] Further, the noncanonical WNT pathway has been associated with pulmonary arterial hypertension as has fractaline and PPAR- γ .^[7,8] Thus, while altered expression of a number of proteins has been shown in patients with IPAH, this may be the “tip of the iceberg.” To date, there have been few proteomic studies that examine the wide range of proteins that may be altered in patients with IPAH.

Using 2D gel electrophoresis with matrix-assisted laser desorption/ionization time-of-flight techniques, Kwapiszewska and colleagues^[9] examined the “early protein changes” of PAH using a hypoxic mouse model and then extended their findings to lungs of patients with IPAH and two rat models of PAH—monocrotaline and hypoxia. Following 24 hours of hypoxia, altered expression of 36 proteins were identified in the mouse lungs. One of the prominently upregulated proteins was identified as four and a half LIM domain protein (Fhl-1), a protein involved in smooth muscle proliferation (changes in LIM expression were highlighted in the study with transformed lymphocytes from patients with HPAH). Immunofluorescence microscopy revealed that the expression of this protein was also increased in the lungs of patients with IPAH, particularly in the plexiform lesions. This paper demonstrates the utility of studies in animal models of PAH, and demonstrates that at least some of the “early changes” of PAH still exist in established PAH.

Histones are basic nuclear proteins responsible for the nucleosome structure of the chromosomal fiber in eukaryotes. Two molecules of each of the four core histones (H2A, H2B, H3, and H4) form an octamer around which wraps approximately 146 bp of DNA in repeating units, called nucleosomes. The linker histone family (H1; currently at least 11 subtypes) functions in the compaction of chromatin into higher order structures. In addition, linker histones play a role in regulation of transcription and more recent studies demonstrate their involvement in protein-protein interactions. While functional redundancy

has been reported between the various subtypes, studies in vertebrates suggest that the various subtypes have specific roles in gene regulation.^[10,11] Whether or not these proteins play a role in the pathogenesis and perpetuation of pulmonary arterial hypertension has not been examined.

The present study used histology-based Matrix-Assisted Laser Desorption Ionization Mass Spectrometry (MALDI MS) to identify protein profiles of pulmonary arteries between 200 and 600 μ m diameter from explanted lungs from patients with IPAH; the purpose was to uncover alterations in expression of the vast array of proteins that may be involved in the pathogenesis of IPAH, and to search for a marker of series of markers of this disease. Unused donor lungs and lung tissue from lobectomy samples served as controls. This technology identified, for the first time, two fragments of histone H1 which were increased in the small arteries when compared to controls; this led to our hypothesis that altered expression of this family of proteins is associated with the pathogenesis of this disease. Paradoxically, confocal microscopy revealed that expression of histone H1 was decreased in the nuclei and suggested an increase in the cytoplasm of arterial cells in IPAH pulmonary arterial walls compared to controls.

MATERIALS AND METHODS

Source of lung tissues

Lung tissue from the explanted right lungs of patients with IPAH ($n = 18$), APAH ($n = 6$), and unused donor lungs ($n = 16$) was harvested by members of the Pulmonary Hypertension Breakthrough Initiative (PHBI). Following excision, the explanted lungs were perfused with saline by way of the pulmonary artery and were inflated with saline by way of the trachea prior to dissection. For this study, lung tissue blocks were cut from various regions of the right lung and snap-frozen in liquid nitrogen. Ten to twelve blocks of lung periphery were examined initially for each case. Snap frozen peripheral lung samples were also obtained from lobectomy samples from Vanderbilt University ($n = 3$; Table 1). The study protocol was approved by the Institutional Research and Ethics Committee of each PHBI site and informed consent was obtained from each patient or their family at the site of surgery and tissue collection. Unique identifiers to conceal identity were assigned to all samples.

Table 1: Data for patients used for histology-based MALDI MS

	Age	Gender	Mean Ppa (Torr)	PGI ₂ therapy	Bosanten	Sildenafil
Controls	37.5±16.4	11/16 Male				
IPAH	34.3±17.6	3/18 Male	58.1±16.1	17/18	13/18	17/18
APAH	49.5±11.0	1/6 Male	52.3±14.8	5/6	6/6	6/6

Data are shown as mean±SEM, **IPAH**: idiopathic pulmonary arterial hypertension; **APAH**: associated pulmonary arterial hypertension; **Ppa**: mean pulmonary artery pressure

Histology-based MALDI

Frozen sections (6 μm thick) were cut from each block and stained with hematoxylin and eosin to identify those blocks containing arterial profiles of arteries between 200 and 600 μm external diameters. In general, five or six blocks of peripheral lung from each case were utilized for further study. The technology of histology-based MALDI MS has been described in detail previously.^[12,13] Briefly, two serial 12 μm frozen sections were cut; one was mounted on a glass slide and stained with hematoxylin and eosin and was scanned using a Mirax Scan digital slide scanner (Mirax, Budapest, Hungary) at a pixel resolution of 0.23 μm , and the other section was mounted on a MALDI target plate and fixed using graded ethanol to remove lipids and salts as well as precipitate the proteins. Arteries of different diameters were marked on the scanned image using a color code, and a 200 μm spot marker applied: <200 μm —yellow; 201–400 μm —green; and 401–600 μm —blue (Fig. 1A). The arteries chosen for marking were those with no obvious hemoglobin in the lumen and with as few associated inflammatory cells as possible. The spotted scanned image and the MALDI plate image were then merged and pixel coordinates of the spots determined for robotic spotting. Matrix spots (20 mg/mL sinapinic acid in 1:1 acetonitrile/0.2% trifluoroacetic acid; 180–220 μm diameter) were placed using an acoustic robotic spotter (LabCyte) on the areas of interest (Fig. 1B). Tissue profile spectra were acquired using an Autoflex II (Bruker Daltonics) MALDI mass spectrometer and run using an automated linear positive-ion mode acquisition method optimized for 2–40 kDa peptides.

Liquid chromatography/mass spectrometry

Portions of intrapulmonary pulmonary artery tissue were excised, extracted with ethanol to reduce the lipid content of the samples, and then re-extracted with 50% acetonitrile,

0.1% TFA to recover the protein fragments. After spinning to remove any debris, the samples were dried to remove the acetonitrile, and then resolubilized in 0.1% formic acid. The mixture was then separated via microflow reversed phase high performance liquid chromatography coupled directly to an LTQ-orbitrap mass spectrometer. This allowed for identification proteins and protein fragments through the combination of both high accuracy masses and their fragmentation patterns.

Immunofluorescent analysis of IPAH and control lung sections

Immunolocalization of histone H1 was performed on paraffin-embedded and frozen sections of human lung tissue obtained from controls and IPAH patients. The IPAH cases with the highest levels of histone H1 fragment expression were selected for further study ($n=5$) together with five random controls. Following deparaffinization, heat-mediated antigen retrieval was performed using a 10 mM citrate buffer (pH 6.0) followed by blocking with 5% normal goat serum. The sections were incubated overnight with primary antibody (histone H1.2, Abcam, Cambridge, Mass.) at 4°C and then reacted with Cy3 labeled secondary antibody (Invitrogen, Carlsbad, Calif.). The slides were mounted using Vectashield mounting media containing DAPI (Vector Laboratories, Burlingame, Calif.) for confocal microscopy and the pictures were digitized. To preserve the relative fluorescence variation, the microscopy settings were the same for all the samples.

Smooth muscle cell isolation and culture

Pulmonary arterial smooth muscle cells (PASMCs) were isolated from distal segments of the left lower lobe of controls ($n = 4$) and IPAH ($n = 4$) lungs, while adherent lung parenchymal tissue was removed using a microscissor and scalpel. The arteries were then

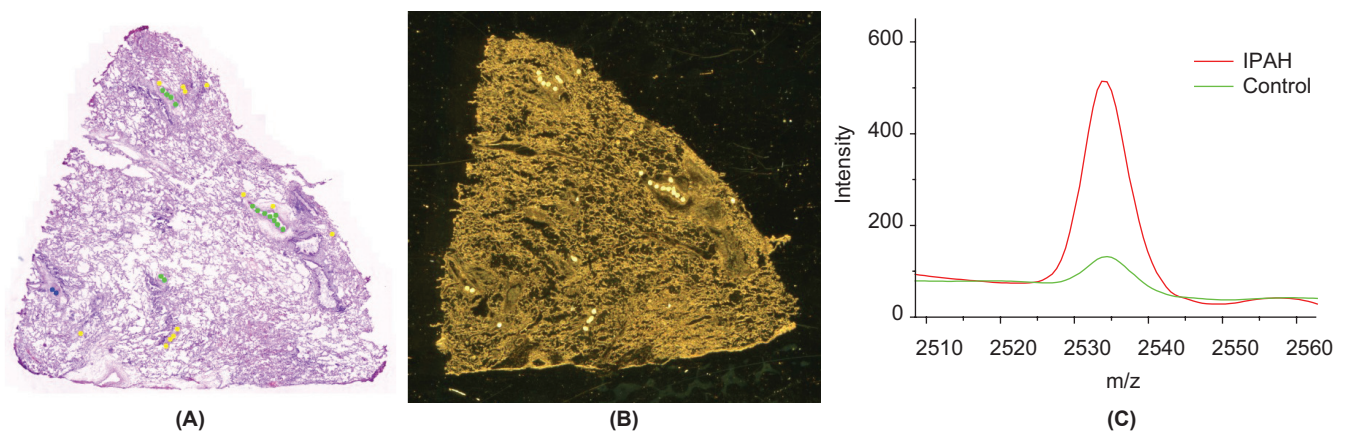


Figure 1: Mass spectral analysis of lung tissues. (A) Annotated stained section of lung tissue. Colors indicate different-size arteries: < 200 μm , yellow; 201–400 μm , green; 401–600 μm , blue. (B) Matrix spotted serial section on a MALDI target. (C) Average mass spectra of IPAH and control showing the intensity difference for the peak at m/z 2535.

minced to 1 mm² blocks with a small drop of medium (SmGm-2 media kit, Lonza). On the following day, culture medium was added to the plate and left undisturbed for three to five days. The medium was changed every other day until the cells reached confluence. Isolated SMCs were characterized by both FACS analysis and immunocytochemistry. For FACS analysis, staining with an α SMA antibody (R&D systems) was used as a marker for SMCs while the endothelial cell marker CD31 antibody (BD Biosciences) was used as a negative control. In addition, antibodies against α SMA (Sigma-Aldrich Co), SM α 22 (AbCam), SMMHC (Abcam) as SMC markers, and CD31 (Neomarkers) as a negative control were used for immunofluorescent analysis. Species-specific antibodies conjugated with Alexa fluor 488 (Invitrogen) were applied following primary antibody incubation to detect positive staining. PSMCs were maintained in SmGM-2 (Smooth Muscle Growth Medium-2) media, and were used between passages 3 and 11.

Nuclear and cytoplasmic protein isolation from PSMCs

For protein extraction from PSMCs, cells were washed to remove serum. Cytoplasmic and nuclear protein fractionation was performed using NE-PER Nuclear and Cytoplasmic extraction kit (Thermo Fisher Scientific, Rockford, Ill.). The protein concentration in the samples was determined by using Bradford assay (Pierce Co., Rockford, Ill.) and was stored at -70°C until use.

Immunofluorescent analysis of histone H1 in PSMC

For localization of histone H1 in PSMCs, 0.5×10^6 cells/mL were plated in Lab-Tex II chamber slides with coverslips (Sigma, St. Louis, Mo.) and incubated overnight. The cells were fixed with 3% paraformaldehyde containing 2% sucrose for 10 min at 37°C followed by permeabilization of the cells (permeabilization buffer: 20 mM HEPES, pH 7.4, 300 mM sucrose, 50 mM NaCl, 3 mM MgCl_2) for 15 min at room temperature. The cells were then incubated with 5% normal goat serum to block the nonspecific antibody binding followed by incubation with primary antibody (histone H1.2 from Abcam [ab17677], Cambridge, Mass.) at 4°C . The sections were visualized with Cy3-labeled secondary antibody (Invitrogen, Carlsbad, Calif.) and mounted using Vectashield mounting media containing DAPI (Vector Laboratories, Burlingame, Calif.) for confocal microscopy. The pictures were digitized, and in order to preserve the relative fluorescence variation the microscopy settings were the same for all samples. Following staining, we determined the number of histone H1-positive nuclei and number of cells with both histone H1-positive nuclei and cytoplasm as a percent of total cells counted in control ($n = 4$) and IPAH ($n = 4$) PSMC cultures. At least 100 cells were counted in each case.

Western blotting of nuclei and cytoplasm from PSMCs

Cytoplasmic and nuclear protein from the PSMCs from IPAH and controls was prepared as above. Ten micrograms of protein was loaded per lane and subjected to SDS-PAGE on 4-12% polyacrylamide gels, and then transferred to nitrocellulose membranes. The blots were blocked for one hour with Odyssey Blocking Buffer (LI-COR Biosciences, Lincoln, Neb.) and probed with primary antibodies (1:1000 dilution in Odyssey Blocking Buffer) histone H1.2 antibody (Abcam, Cambridge, Mass.), importin β (Abcam, Cambridge, MA) or importin 7 (Santa Cruz Biotechnology Inc., Santa Cruz, Calif.). The following day, blots were washed in TBS containing 0.1% Tween 20, incubated for one hour with secondary antibodies (IRDye 800 CW-conjugated), washed again, and scanned for infrared signal using the Odyssey Imaging System (LI-COR Biosciences). The blot with cytoplasmic protein was reprobed with β -microglobulin antibody (Santa Cruz Biotech, Santa Cruz, Calif.) as a loading control.

Association of histone H1 with importin β and importin 7

For immunoprecipitation, 100 mg of cytoplasmic and nuclear protein from control and IPAH PSMCs was incubated with histone H1 antibody (Santa Cruz Biotechnology Inc. [sc-10806], Santa Cruz, Calif.) in immunoprecipitation buffer (20 mM Tris pH 7.75, 1% Triton, 0.5% deoxycholate, 0.15 M NaCl, 0.02% sodium azide and 0.34 TIU/mL aprotinin) overnight at 4°C . The following day, protein A agarose beads (20 μl of 50% bead slurry; Sigma, St. Louis, Mo.) were added and incubated for two hours at 4°C . The pellet was washed with RIPA buffer (10 mM Tris pH 8.6, 1 mM EDTA, 1% Triton, 1% deoxycholate, 0.15 M NaCl, 0.1% SDS), resuspended with 20 μl 3 \times SDS sample buffer, and heated to $95-100^{\circ}\text{C}$ for five minutes before analyzing the samples by Western blotting using importin β (Abcam, Inc [ab45938], importin 7; Santa Cruz Technology, Inc. [sc-365231]) and histone H1 antibodies.

MNase digestion

Pellets of PSMCs were dissolved in buffer A (10 mM Tris-HCl pH 7.4, 10 mM NaCl, 3 mM MgCl_2 , 0.3 M sucrose and 0.2 mM PMSF) plus 0.2% of NP40 and were incubated for 10 min at 4°C . Nuclei were obtained after centrifugation and digested with eight units of MNase (per eight million of nuclei for five minutes at room temperature in buffer A plus 10 mM CaCl_2). The resultant DNA was purified through a Qiagen column and run on 2% agarose gel.^[14]

Statistical analyses

A pilot study of 11 IPAH cases, 6 APAH cases, and 12 controls revealed that the alteration in protein expression in the IPAH and APAH were similar. For this reason, in a second

proof of concept set of cases, additional cases were added only to the IPAH and control cases giving a total of 18 IPAH and 16 control cases. The MALDI MS data of protein expression from all cases were preprocessed in the following steps: (1) calibration; (2) baseline correction; (3) deionizing; (4) normalization; (5) peak detection; and (6) quantification. For each set of data for arteries of each size range, we identified a number of proteins together as a classifier to distinguish between IPAH and control lung samples. The selection of the discriminatory proteins was based on the statistical significance of false discovery rate (FDR)-controlled P -value < 0.1 for the t test, Wilcoxon's test, and Kolmogorov-Smirnov test, and > 2 for the significance analysis of microarrays (SAM). The weighted flexible compound covariate method (WFCCM) was used to summarize the protein expression associated with the biological status from each analysis method, and the selected proteins were reduced to one summarized risk score for each patient. The class prediction performance was assessed by the leave-one-out cross-validation method. The preprocessing was carried out using the MATLAB package Wavespec.

Statistical analysis of cell studies

Statistical analyses for immunolocalization of histone H1 in PASMCs and densitometric analysis of protein bands following Western analysis and immunoprecipitation studies were carried out using unpaired two-tailed t tests (GraphPad Prism Software, La Jolla, Calif.). Data are expressed as mean \pm SEM. A $P < 0.05$ was considered significant.

Statistical analysis of Mnase digestion

NRL analysis was carried out using NIH ImageJ. Data were analyzed by two-way ANOVA and Bonferroni posttest. Data are expressed as mean + SEM.

RESULTS

Histology-directed MALDI MS of pulmonary arteries

Using histology-directed MALDI MS, we analyzed 12- μ m-thick frozen sections of the pulmonary arteries from 18 IPAH, 6 APAH, and 16 control lungs. Mass spectra from the pulmonary arteries were grouped into the following arterial diameter-size ranges: $< 200 \mu\text{m}$; $201\text{--}400 \mu\text{m}$; and $401\text{--}600 \mu\text{m}$. Statistical analyses revealed several proteins (as yet unidentified) that were statistically different between the IPAH cases and controls at each arterial level. The changes in protein expression in the APAH cases, in general, trended with those in the IPAH cases (data not shown). A major protein that was identified was histone H1; two fragments of this protein were identified, one by MASCOT following MALDI MS/MS (m/z 2535), and a second fragment (m/z 2140) by LC-MS (Table 2). In the IPAH cases, both of these fragments were significantly increased above control levels (Figures 1C and 2). The fragments were naturally occurring as no enzymes were used during the histology-directed MALDI MS. The peptide sequences for these two fragments were identical to sequences for histone H1.2 (NP_005310.1), 1.3 (NP_005311.1), 1.4 (NP_005312.1), and 1.5 (NP_005313.1); they ran concurrently with m/z 2140

Table 2: Peptide sequence of histone H1 and identified fragments

	Fragment m/z 2140	Fragment m/z 2535	
			kasgppv selitkavaa skersgvsla alkkalaaag ydveknnsr
Histone H1.2	21 kkaakkag	tprkasgppv selitkavaa skersgvsla alkkalaaag ydveknnsri	klglkslvsk 90
Histone H1.3	21 kkkakkagat	agkrkasgppv vselitkava askersgvsla alkkalaaag ydveknnsri	klglkslvsk 90
Histone H1.4	21 kkkarksaga	akrkasgppv selitkavaa skersgvsla alkkalaaag ydveknnsri	klglkslvsk 90
Histone H1.5	21 atkkaagaga	akrkatgppv selitkavaa skernglsla alkkalaaag ydveknnsri	klglkslvsk 90

Mismatches in peptide sequence of histone H1.5 are bolded

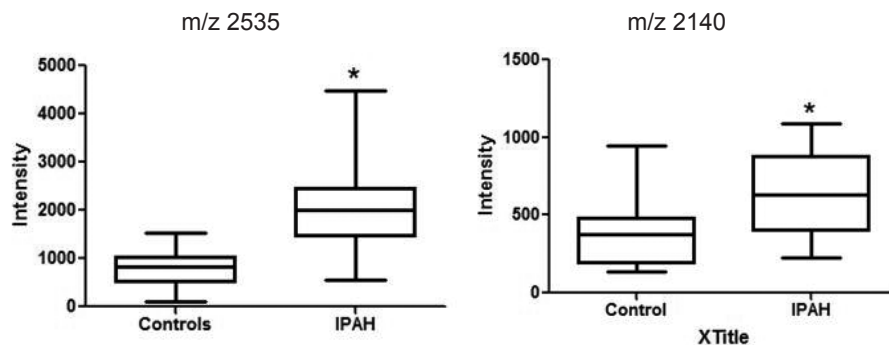


Figure 2: Intensities of the two fragments of histone H1 in control (open box) and IPAH (black box) pulmonary arteries. The fragment with a mass to charge (m/z) of 2140 was identified by LC-MS and the second fragment (m/z 2535) was identified by MALDI MS directly from the tissue section and MASCOT searching. Data are mean + SEM; * $P < 0.05$ when IPAH compared to controls.

immediately preceding m/z 2535 (Table 2). Only fragment m/z 2535 was identified in histone H1.1 (NP_005316.1). These data demonstrate that fragmentation of histone H1 occurs more frequently in the pulmonary arteries from IPAH cases than in those from controls.

Immunolocalization of histone H1 in IPAH and control pulmonary arteries

Using an antibody to histone H1, we performed immunofluorescence analyses on paraffin-embedded lung tissue from both controls and IPAH patients to determine cellular localization histone H1. In control pulmonary arteries, histone H1 localized predominantly in the nucleoli with some reactivity in the cytoplasm in both endothelial cells (PAECs) as well as smooth muscle cells (PASMCs; Fig. 3). A striking decrease in localization of H1 in the nucleus of both cell types was observed in the IPAH arteries when compared to controls (Fig. 3). A small increase in histone H1 expression was apparent in the cytoplasm of some of the IPAH cases as compared to controls (Fig. 3).

To determine whether the decreased expression of histone H1 in the paraffin-embedded arteries was the result of processing, we next examined the arteries in frozen sections. As seen in the paraffin sections, the frozen sections revealed that nuclear localization of histone H1 was decreased in the pulmonary artery smooth muscle and endothelial cells from the IPAH cases compared to controls, while expression of histone H1 in the cytoplasm of these cells was increased and clustered mainly in the perinuclear regions when compared to controls (Fig. 4). These findings confirm the significant decrease in nuclear and increase in cytoplasmic localization

of histone H1 in the cells of the pulmonary artery walls in IPAH.

Immunolocalization of histone H1 in cultured IPAH and control PASMCs

The nuclear and cytoplasmic localization of histone H1 was confirmed in cultured pulmonary PASMCs from control and IPAH samples by confocal microscopy. While in control PASMCs a strong histone H1 signal was apparent in the nucleoli, this signal was strikingly reduced in the IPAH PASMCs (Figures 5A and B). Quantitation of the percent of nuclei showing strong nuclear localization confirmed this finding; this demonstrated that approximately 80% of control cells showed strong histone H1 immunoreactivity, while this number was reduced to approximately 20% in the IPAH cells (Fig. 5C). These cells also demonstrated cytoplasmic localization of histone H1. Counts of the number of cells showing only cytoplasmic reactivity revealed a significant increase in the IPAH cells compared to controls (Fig. 5D). As seen in the frozen sections, the cytoplasmic histone H1 was found mainly in the perinuclear region. These data reflect the findings in lung tissue.

Nuclear and cytoplasmic expression of histone H1 in IPAH and control PASMCs—western analysis

Using nuclear and cytoplasmic protein fractions from cultured control and IPAH PASMCs we performed Western analyses to confirm our immunofluorescence findings. Western analyses revealed histone H1 expression in both the cytoplasm and nucleus of control PASMCs (Fig. 6). In IPAH PASMCs, the expression of histone H1 was strikingly decreased in the nuclear fraction compared to controls (50% reduction) while in the cytoplasm, histone H1 expression was significantly increased.

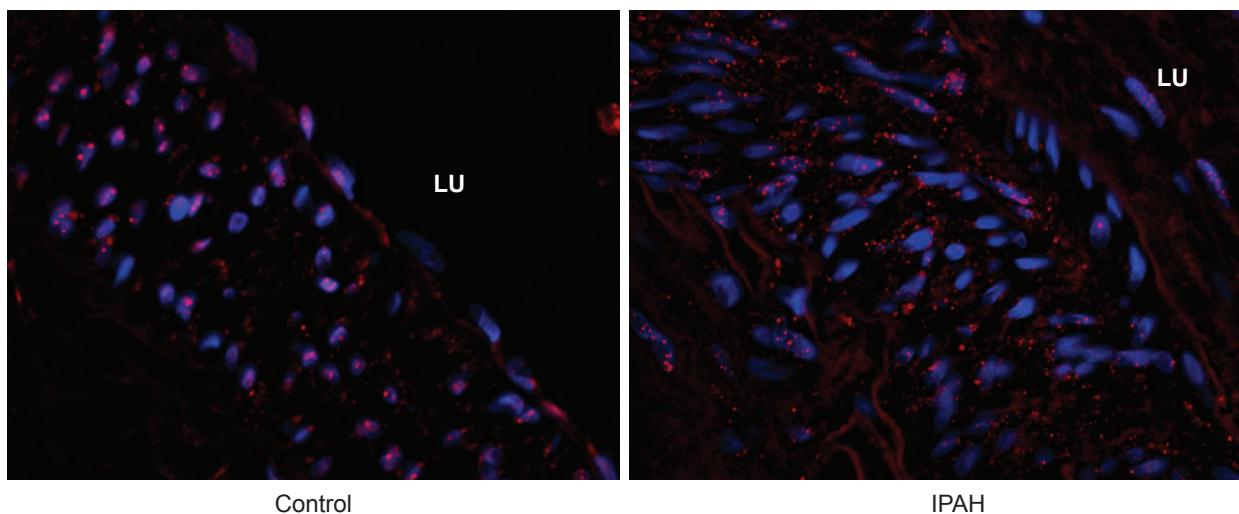


Figure 3: Confocal image of paraffin-embedded sections of pulmonary artery stained with an antibody to histone H1 (red to pink) and counterstained with DAPI (blue). In control endothelial and smooth muscle cells, the histone H1 is located mainly in the nuclei giving a pink coloration. Little staining is apparent in the cytoplasm. Endothelial and smooth muscle cells of the IPAH artery show little localization of histone H1 in the nuclei but cytoplasmic staining is more abundant than in control. Lumen (Lu) X.

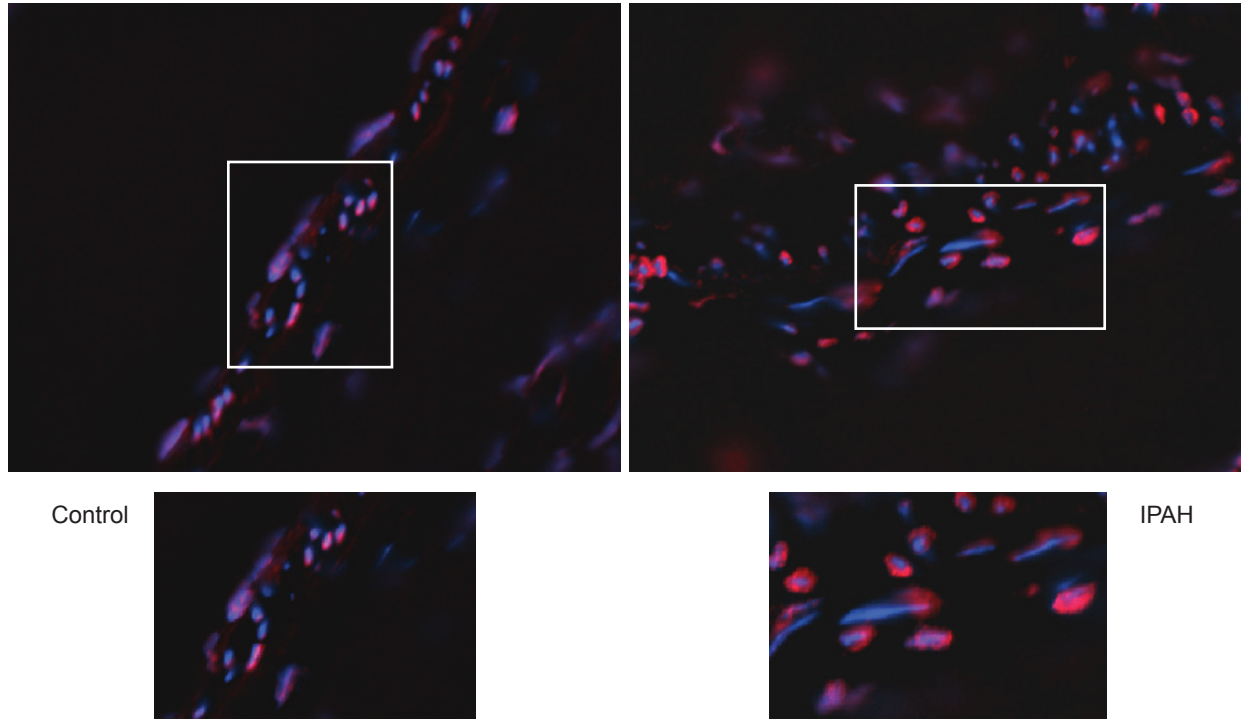


Figure 4: Confocal microscopy of frozen sections of control and IPAH pulmonary arteries treated with an antibody to histone H1 (red to pink) and counterstained with DAPI (blue). X

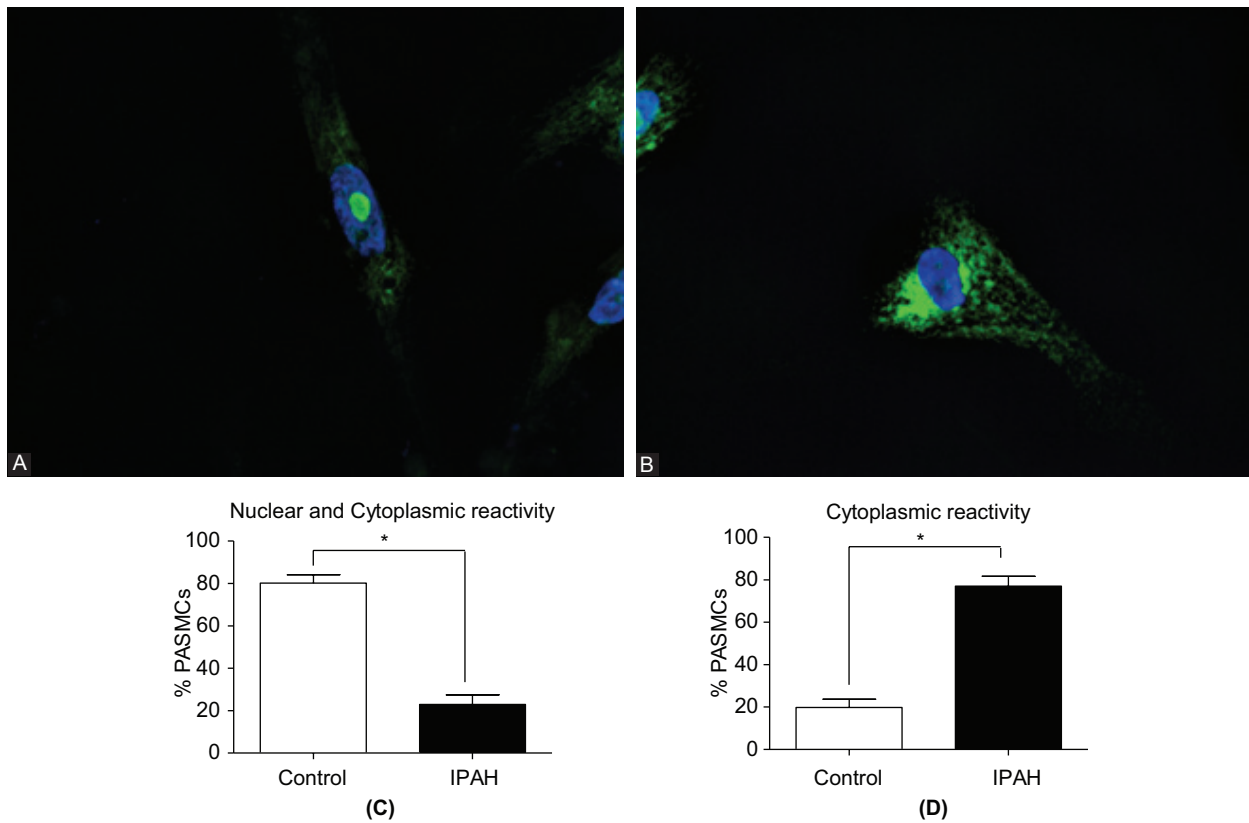


Figure 5: Confocal micrographs showing (A) strong nucleolar localization of histone H1 (green) in the nucleus of controls PASMCs with little cytoplasmic reactivity. In contrast, strong cytoplasmic immunoreactivity is apparent in the IPAH cells with little in the nucleus (B). Nuclear staining with DAPI: blue. (C) Percent of PASMCs showing nuclear and cytoplasmic histone H1 immunoreactivity in control (open bars) and IPAH cells (closed bars). (D) Percent of PASMCs showing cytoplasmic immunoreactivity in control and IPAH cells.

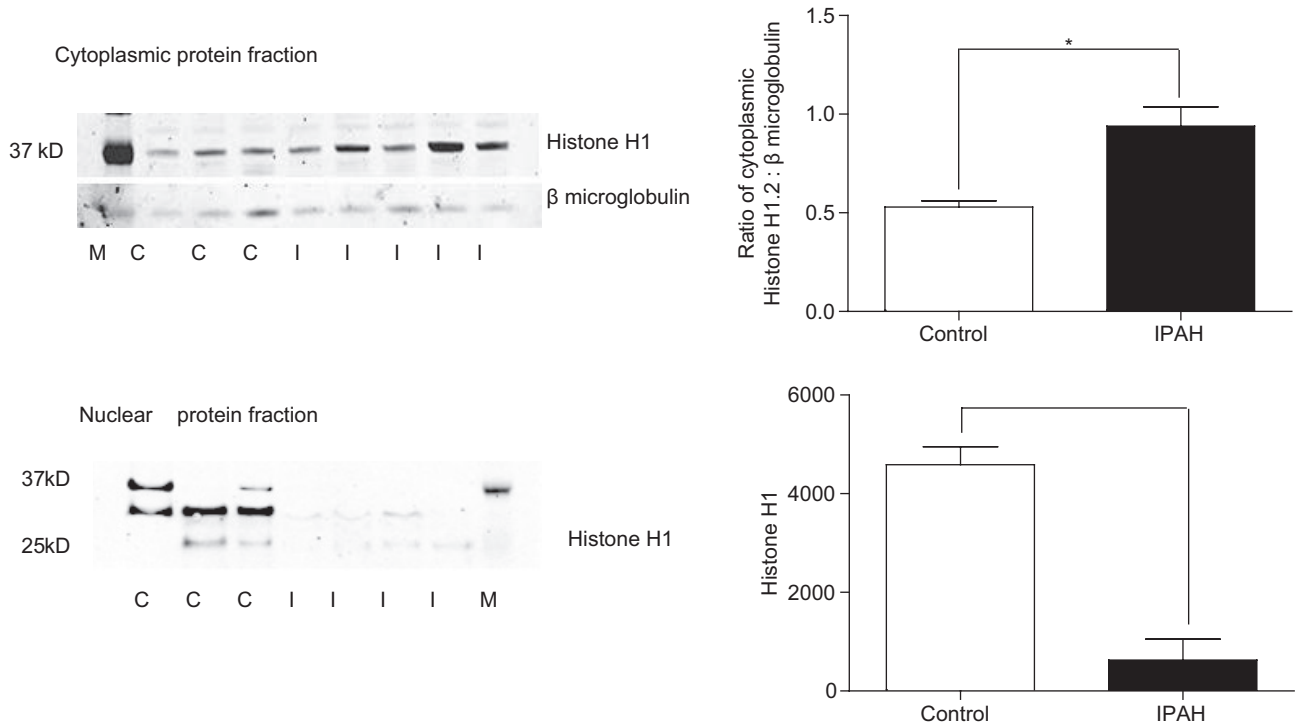


Figure 6: Representative western blots of cytoplasmic and nuclear fractions of control and IPAH PSMCs. Histone H1 expression was significantly increased in the IPAH cells compared to controls. Nuclear histone H1 expression was significantly reduced in the IPAH nuclear fraction compared to controls. Densitometric data for histone H1 is related to β microglobulin. A total of three control different cell lines and four IPAH cells lines were examined. Data are shown as mean + SEM; * $P < 0.05$.

Does the reduction in histone H1 in the nucleus reflect an alteration in importins?

Two importins have been shown to be responsible for the transport of linker histones from the cytoplasm to the nucleus—importin β and importin 7. Both importins separately interact with H1, but only as a dimer do they facilitate the translocation into the nucleus. We wondered whether the transport of linker histones into the nucleus following their synthesis in the cytoplasm is decreased because of alterations in the interaction of histone H1 with the two importins. In control and IPAH PSMCs, histone H1 was immunoprecipitated from the cytoplasmic and nuclear protein fractions followed by immunoblotting with either importin β or importin 7 antibodies. Importin β and importin 7 associated with histone H1 in both the control and IPAH PSMCs in both the nuclear and cytoplasmic fractions. In IPAH PSMCs, the cytoplasmic association of histone H1 with importin β was significantly decreased, whereas the nuclear association of histone H1 with importin β was similar to controls (Fig. 7A). This suggests that, in IPAH PSMCs, formation of histone H1 complexes with importin β in the cytoplasm is diminished. In control and IPAH PSMCs, there was no difference in binding of histone H1 to importin 7 in either the cytoplasmic or nuclear fractions (Fig. 7B).

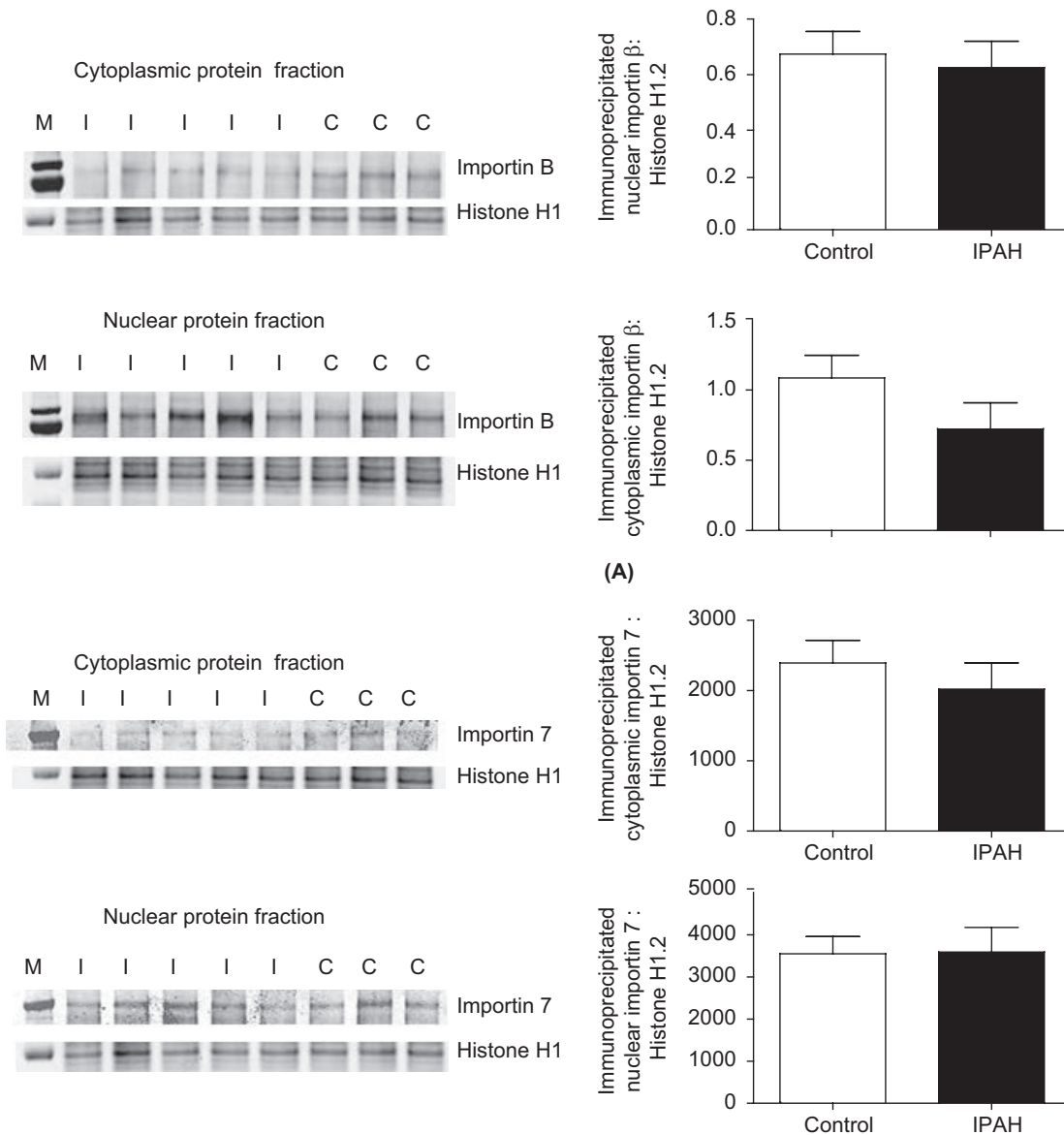
MNase protection

Since the expression of histone H1 is reduced in the IPAH

PASMCs compared to controls and the chromosome pattern in the nucleoli is less compact, we wondered whether the nucleosome repeat length (NRL) would be altered. Micrococcal nuclease digestion of bulk chromatin from PSMCs revealed an ~ 20 bp increase in the spacing between the nucleosomes (NRL) of the IPAH cells ~ 171 versus the controls ~ 191 (Fig. 8). These data suggest that the IPAH cells have a more open reading frame in the nucleoli than the control cells.

DISCUSSION

Using histology-directed MALDI MS and LC-MS, the present study identified two fragments of histone H1 that are significantly increased in pulmonary arteries (200 and 600 μ m diameter) in explanted lungs from patients with IPAH compared to controls. Paradoxically, confocal microscopy revealed that expression of histone H1 was decreased in the nuclei; additionally, the nucleoli were less condensed in appearance in endothelial and smooth muscle cells of small pulmonary arteries in IPAH lungs compared to controls, while histone H1 expression in the cytoplasm seemed increased. Western blot analysis of nuclear and cytoplasmic fractions of cultured PSMCs confirmed the reduction in histone H1 expression in the nuclei of IPAH PSMCs compared to control cells and the significant increase in the cytoplasmic fraction.



Figures 7: Western analyses of (A) importin β and (B) importin 7 in cytoplasmic and nuclear protein fractions of control (C) and IPAH (I) PSMCs following precipitation with an antibody to histone H1. Expression of importin β is significantly reduced in the cytoplasmic fraction compared to controls; expression in the nuclear fraction was similar in both groups. Expression of importin 7 was similar in controls and IPAH cells for both importin β and importin 7. Data are related to histone H1 expression and are shown as $m \pm SEM$. * $P < 0.05$.

Immunoprecipitation studies revealed a significant reduction in the association of histone H1 with importin β (one of the transporter proteins responsible for the translocation of histone H1 into the nucleus), but not with importin 7 in the cytoplasmic fraction of IPAH PSMCs when compared to controls; association of both importins to histone H1 in the nucleus was similar in IPAH and control groups. Calculation of nucleosomal repeat length in bulk chromatin revealed that the space between chromosomes was strikingly increased in the IPAH compared to control PSMCs (~ 20 bp).

Histology-directed MALDI MS has not previously been utilized to directly unravel the changes in protein expression in pulmonary arteries of IPAH patients. Label-free liquid

chromatography tandem mass spectrometry has been used to compare protein profiles in surgical lung tissue from PAH patients ($n = 8$) versus controls ($n = 8$).^[15] In that study, 25 proteins were highlighted that exhibited different levels of protein expression. These proteins were associated mainly with proliferation, cell growth, and cell metabolism. Of the identified proteins, annexin A3, CLIC1, and four-and-a-half LIM domains protein 1 expression had been previously linked to the hypoxia and monocrotaline models of PAH;^[9,16] furthermore, periostin has linked to pulmonary arteries in chronic hypoxic rat.^[17] The design of that study was such that the protein profiles examined were from all regions of the peripheral lung, making interpretation of the data difficult to attribute to the pulmonary arteries. Our study was

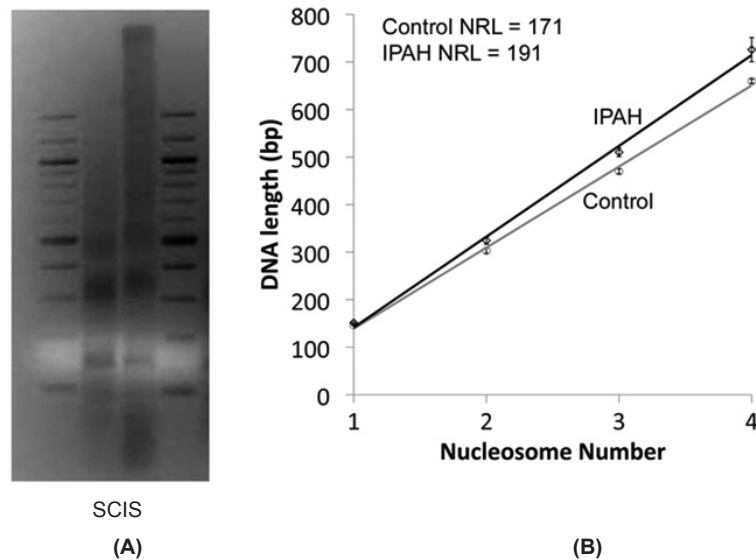


Figure 8: (A) Nuclei of control (C) and IPAH (I) PASMCS treated with MNase and profile of bulk chromatin analyzed by gel electrophoresis to allow calculation of nucleosome repeat length (NRL). S = standard. (B) Plot of nucleosome number against DNA length for bulk chromatin from control ($n = 3$) and IPAH ($n = 3$) PASMCS. Controls show a nuclear repeat length (NRL) of 171 while that of the IPAH samples show an NRL of 191. Data are mean + SEM, $*P < 0.05$.

specifically designed to detect changes in the protein profiles in small pulmonary arteries from control and IPAH cases. A further difference of note between their study and ours is that LC-MS requires homogenization of the tissue; therefore, only the bulk properties of the sample were determined. In comparison, our study used a targeted approach which enabled determination of molecular changes in individual arteries. While several caveats arise from our study (i.e., severity of disease in explanted lungs, use of vasodilator therapy in IPAH patients, and failure to identify most of the proteins identified as altered) a significant increase in two fragments of the linker histone H1 protein in the IPAH arteries when compared to controls proved to be a striking and reproducible change.

Linker histones are best known for their ability to bind to nucleosomes and stabilize both nucleosomes and condensed higher order chromatin structures.^[18] As expected, our study showed the expression of histone H1 in the nuclei of PASMCS and PAECs of control lungs. However, in IPAH arterial tissue, the localization of histone H1 was strikingly reduced in the nuclei, and the nucleoli appeared less condensed than in controls. These findings were recapitulated in cultured PASMCS from control and IPAH cases. Whether or not our findings of reduced nuclear localization of histone H1 and less condensed chromatin pattern in IPAH reflect the fragmentation of histone H1 is not certain and requires further study. Depletion of histone H1 in the nucleus is known to alter chromatin structure.^[14]

Alternatively, the reduction in nuclear histone H1 and the less dense chromatin pattern could be a reflection of the increased nucleosomal repeat length found in the IPAH

PASMCS. However, earlier studies have, in general, associated a loss of histone H1 with decreased nucleosomal repeat length.^[19,20] In contrast, Laitinen et al. reported an increased nucleosomal repeat length in association with decreased histone H1 in oncogene-transformed NIH 3T3 fibroblasts;^[21] our results are in agreement with this finding. The reason for the differences in findings between our study and Laitinen et al. may lie in our use of human primary cell lines and our comparison of cells from normal and diseased tissues.

Recently, linker histones have also been found to contribute to many other cellular processes. For example, linker histones have been found to play a role in transcription,^[21-23] gene regulation,^[14] protein-protein interactions,^[11] innate immunity,^[24] and as a complex to downregulate proinflammatory genes.^[25] Furthermore, post-translational modifications of histone H1 have been linked to specific functions in particular cell types.^[26] Whether the reduced nuclear histone H1 expression can be linked to the various changes outlined above can only be speculated at present and require further study. Our finding of the increased length between chromosomes in IPAH suggests a more open reading frame,^[18,27,28] which may contribute to the alterations in protein expression seen in IPAH.

The present data found a significant increase in expression of histone H1 in the cytoplasm. Conventionally, linker histones are present in the cytoplasm when the cell undergoes apoptosis. For example, DNA double-strand breaks induce translocation of nuclear H1 to the cytoplasm where it promotes release of cytochrome c from mitochondria by activating the Bcl-2 family protein Bak.^[29] However, examination of apoptosis in both IPAH and control lungs,

using TUNEL staining and an antibody to phosphohistone H2B, failed to show any increase in apoptosis (data not shown). Cytoplasmic pools of histone H1 have previously been shown in mammalian cells.^[24,30]

The increased fragmentation of histone H1 in the IPAH pulmonary arteries demonstrated by histology-based MALDI MS may, at least in part, explain the reduced expression of histone H1 in the nucleus. Alternatively, it is possible that the antibody fails to bind securely to the small fragment of histone H1 resulting in an apparent reduction in histone H1 expression. This seems unlikely since the nuclear chromatin pattern is also altered in the IPAH cases. It is also possible that the reduction in nuclear histone H1 is the result of a failure of the cytoplasmic importins to recognize the H1 fragments and thus they are not ferried into the nucleus.

Under normal circumstances, newly synthesized cytoplasmic linker histones are imported into the nucleus through an energy-dependent process mediated by an importin β -importin 7 heterodimer. Importin β is the most efficient import receptor for the globular domain of H1 histones, while importin 7 plays a more passive role resembling an import adapter.^[31] The heterodimer of importin β -importin 7 is the functional receptor for the entire C-terminal domain and is the only receptor for H1 import.^[31,32] In control PSMCs, we demonstrated an association of importin β and importin 7 with histone H1 in both the cytoplasmic and nuclear fractions. However, in the IPAH PSMCs, the cytoplasmic association of histone H1 with importin β was significantly decreased. This finding may reflect a weak interaction between histone H1 and importin β and/or that the fragmented histone H1 in IPAH is unable to dimerize with importin β . While we found no difference in the interaction of importin 7 with histone H1, previous studies have found that a heterodimer of both importins is essential for import. Thus, our studies suggest that the reduction of nuclear histone H1 may reflect its reduced interaction with importin β . The fragmentation of histone H1 also likely contributes to the reduced interaction.

In summary, our results demonstrate alterations in histone H1 expression in the cells of the pulmonary arteries in patients with IPAH. The expression of histone H1 is altered in both the cytoplasm and nuclei of IPAH pulmonary arteries and PSMCs and is accompanied by a less dense appearance of the nucleoli. Our results also suggest that importation of histone H1 into the nucleus is impaired perhaps because of both the fragmentation of histone H1 and a decrease in association of histone H1 to importin β . Finally, our data suggest a link between a reduction in the expression of nuclear histone H1 and an increase in nucleosomal repeat length. We further suggest that,

in IPAH, the decreased nuclear H1 contributes the less compact nucleosomal pattern and this, in turn, contributes to the increase in NRL and ultimately to changes in transcription. Further studies are needed to support this notion.

ACKNOWLEDGMENTS

Lung tissues from IPAH and APAH patients and control subjects were provided by the Pulmonary Hypertension Breakthrough Initiative (PHBI). Lung tissues were procured at the Transplant Procurement Centers at Stanford University (Dr. Marlene Rabinovitch, M.D.), University of California at San Diego (Patricia Thistlethwaite, M.D., Ph.D.), The Cleveland Clinic (Serpil Erzarum, M.D.), University of Alabama, Birmingham (Dr. Keith Willie), Baylor College of Medicine (George Noon, M.D.), Duke University Medical Center (Jerry Eu, M.D.), University of Michigan (Douglas Arenberg, M.D.), Allegheny General Hospital (Raymond Benza, M.D.) and Vanderbilt University (Barbara Meyrick, Ph.D.). Paraffin sections were provided by Rubin Tudor, M.D., University of Colorado, patient data was provided by the Data Bank and Coordinating Center, University of Michigan (Valerie McLaughlin, M.D.) and tissue from the various Procurement Centers was provided via the Tissue Processing Center, University of Alabama, Birmingham (William Grizzle, M.D.). Drs. K. Ihida-Stansbury and H. Delisser are members of the PHBI Cell Center. Jamie Allen is thanked for her assistance with sample preparation.

REFERENCES

1. Meyrick B. The pathology of pulmonary artery hypertension. *Clin Chest Med* 2001;22:393-404.
2. Stenmark KR, Meyrick B, Galie N, Mooi WJ, McMurry IF. Animal models of pulmonary arterial hypertension: the hope for etiological discovery and pharmacological cure. *Am J Physiol Lung Cell Mol Physiol* 2009;297:L1013-32.
3. Tudor RM, Chacon M, Alger L, Wang J, Taraseviciene-Stewart L, Kasahara Y, et al. Expression of angiogenesis-related molecules in plexiform lesions in severe pulmonary hypertension: evidence for a process of disordered angiogenesis. *J Pathol* 2001;195:367-74.
4. Wright L, Tudor RM, Wang J, Cool CD, Lopley RA, Voelkel NF. 5-Lipoxygenase and 5-lipoxygenase activating protein (FLAP) immunoreactivity in lungs from patients with primary pulmonary hypertension. *Am J Respir Crit Care Med* 1998;157:219-29.
5. Jones PL, Crack J, Rabinovitch M. Regulation of tenascin-C, a vascular smooth muscle cell survival factor that interacts with the alpha v beta 3 integrin to promote epidermal growth factor receptor phosphorylation and growth. *J Cell Biol* 1997;139:279-93.
6. Jones PL, Rabinovitch M. Tenascin-C is induced with progressive pulmonary vascular disease in rats and is functionally related to increased smooth muscle cell proliferation. *Circ Res* 1996;79:1131-42.
7. Balabanian K, Foussat A, Dorfmueller P, Durand-Gasselini I, Capel F, Bouchet-Delbos L, et al. CX(3)C chemokine fractalkine in pulmonary arterial hypertension. *Am J Respir Crit Care Med* 2002;165:1419-25.
8. Ameshima S, Golpon H, Cool CD, Chan D, Vandivier RW, Gardai SJ, et al. Peroxisome proliferator-activated receptor gamma (PPARgamma) expression is decreased in pulmonary hypertension and affects endothelial cell growth. *Circ Res* 2003;92:1162-9.
9. Kwapiszewska G, Wygrecka M, Marsh LM, Schmitt S, Trösser R, Wilhelm J, et al. Fhl-1, a new key protein in pulmonary hypertension. *Circulation* 2008;118:1183-94.
10. Happel N, Doenecke D. Histone H1 and its isoforms: contribution to chromatin structure and function. *Gene* 2009;431:1-12.
11. McBryant SJ, Lu X, Hansen JC. Multifunctionality of the linker histones: an emerging role for protein-protein interactions. *Cell Res* 2010;20:519-28.
12. Schwartz SA, Reyzer ML, Caprioli RM. Direct tissue analysis using

- matrix-assisted laser desorption/ionization mass spectrometry: practical aspects of sample preparation. *J Mass Spectrom* 2003;38:699-708.
13. Cornett DS, Mobley JA, Dias EC, Andersson M, Arteaga CL, et al. A novel histology-directed strategy for MALDI-MS tissue profiling that improves throughput and cellular specificity in human breast cancer. *Mol Cell Proteomics* 2006;5:1975-83.
 14. Fan Y, Nikitina T, Zhao J, Fleury TJ, Bhattacharyya R, Bouhassira EE, et al. Histone H1 depletion in mammals alters global chromatin structure but causes specific changes in gene regulation. *Cell* 2005;123:1199-212.
 15. Abdul-Salam VB, Wharton J, Cupitt J, Berryman M, Edwards RJ, Wilkins MR. Proteomic analysis of lung tissues from patients with pulmonary arterial hypertension. *Circulation* 2010;122:2058-67.
 16. Laudi S, Steudel W, Jonscher K, Schöning W, Schniedewind B, Kaisers U, et al. Comparison of lung proteome profiles in two rodent models of pulmonary arterial hypertension. *Proteomics* 2007;7:2469-78.
 17. Li P, Oparil S, Feng W, Chen YF. Hypoxia-responsive growth factors upregulate periostin and osteopontin expression via distinct signaling pathways in rat pulmonary arterial smooth muscle cells. *J Appl Physiol* 2004;97:1550-8.
 18. Szerlong HJ, Hansen JC. Nucleosome distribution and linker DNA: Connecting nuclear function to dynamic chromatin structure. *Biochem Cell Biol* 2011;89:24-34.
 19. Bates DL, Thomas JO. Histones H1 and H5: one or two molecules per nucleosome? *Nucleic Acids Res* 1981;9:5883-94.
 20. Woodcock CL, Skoultchi AI, Fan Y. Role of linker histone in chromatin structure and function: H1 stoichiometry and nucleosome repeat length. *Chromosome Res* 2006;14:17-25.
 21. Laitinen J, Sistonen L, Alitalo K, Holtta E. Cell transformation by c-Ha-rasVal12 oncogene is accompanied by a decrease in histone H1 zero and an increase in nucleosomal repeat length. *J Cell Biochem* 1995;57:1-11.
 22. Clayton AL, Hazzalin CA, Mahadevan LC. Enhanced histone acetylation and transcription: a dynamic perspective. *Mol Cell* 2006;23:289-96.
 23. Sancho M, Diani E, Beato M, Jordan A. Depletion of human histone H1 variants uncovers specific roles in gene expression and cell growth. *PLoS Genet* 2008;4:e1000227.
 24. Parseghian MH, Luhrs KA. Beyond the walls of the nucleus: The role of histones in cellular signaling and innate immunity. *Biochem Cell Biol* 2006;84:589-604.
 25. El GM, Yoza BK, Chen X, Garcia BA, Young NL, McCall CE. Chromatin-specific remodeling by HMGB1 and linker histone H1 silences proinflammatory genes during endotoxin tolerance. *Mol Cell Biol* 2009;29:1959-71.
 26. Wood C, Snijders A, Williamson J, Reynolds C, Baldwin J, Dickman M. Post-translational modifications of the linker histone variants and their association with cell mechanisms. *FEBS J* 2009;276:3685-97.
 27. O'Neill TE, Meersseman G, Pennings S, Bradbury EM. Deposition of histone H1 onto reconstituted nucleosome arrays inhibits both initiation and elongation of transcripts by T7 RNA polymerase. *Nucleic Acids Res* 1995;23:1075-82.
 28. Kim A, Dean A. A human globin enhancer causes both discrete and widespread alterations in chromatin structure. *Mol Cell Biol* 2003;23:8099-109.
 29. Gillespie DA, Vousden KH. The secret life of histones. *Cell* 2003;114:655-6.
 30. Zlatanova JS, Srebrena LN, Banchev TB, Tasheva BT, Tsanev RG. Cytoplasmic pool of histone H1 in mammalian cells. *J Cell Sci* 1990;96:461-8.
 31. Jäkel S, Albig W, Kutay U, Bischoff FR, Schwamborn K, Doenecke D, et al. The importin beta/importin 7 heterodimer is a functional nuclear import receptor for histone H1. *EMBO J* 1999;18:2411-23.
 32. Bauerle M, Doenecke D, Albig W. The requirement of H1 histones for a heterodimeric nuclear import receptor. *J Biol Chem* 2002;277:32480-9.

Source of Support: The Pulmonary Hypertension Breakthrough Initiative of the Cardiopulmonary Medical Research and Education Fund and grants from the National Center for Research Resources (5P41RR031461-02) and the National Institute of General Medical Sciences (8 P41 GM103391-02) from the National Institutes of Health., **Conflict of Interest:** None declared.

Announcement

iPhone App



Download
iPhone, iPad
application

FREE

A free application to browse and search the journal's content is now available for iPhone/iPad. The application provides "Table of Contents" of the latest issues, which are stored on the device for future offline browsing. Internet connection is required to access the back issues and search facility. The application is Compatible with iPhone, iPod touch, and iPad and Requires iOS 3.1 or later. The application can be downloaded from <http://itunes.apple.com/us/app/medknow-journals/id458064375?ls=1&mt=8>. For suggestions and comments do write back to us.